Refereed Proceedings

Heat Exchanger Fouling and Cleaning: Fundamentals and Applications

Engineering Conferences International *Year* 2003

The Early Stages of Deposition of Magnetite Particles onto Alloy-800 Heat Exchange Surfaces under Subcooled Boiling Conditions

Norman Arbeau
University of New Brunswick

William Cook
University of New Brunswick

Derek Lister
University of New Brunswick

Norman Arbeau, William Cook and Derek Lister

arbeau@unb.ca, wcook@unb.ca, dlister@unb.ca
Department of Chemical Engineering, University of New Brunswick
PO Box 4400, Fredericton, NB, Canada, E3B 5A3

ABSTRACT

The data collected during experiments in water loops on the fouling of heat exchange surfaces with magnetite particles often display a dip in the deposit accumulation curve at about 10 – 20 hours into the experiment. Generally the dips are small enough to be considered part of the scatter and may not even be discernible in long runs with considerable amounts of deposit. We have examined this phenomenon in a series of short experiments lasting up to a maximum of 40 hours. The test section of the recirculating water loop used for the study contained a heat exchanger tube of Alloy-800. Synthetic magnetite colloids were suspended in the coolant, which was usually maintained at 60°C or 90°C, and their deposition onto the tube was monitored for different conditions of pH, flow rate and heat flux. For a pH where deposition should be dominated by transport processes, deposition curves all displayed a "knee" at about 5 – 10 hours, regardless of whether the tube was heated or not. The curve shape can be explained in terms of a layered growth of the deposit, the first layer conditioning the surface for the growth of subsequent layers. First-order phenomenological coefficients in a simple model reproduce the curves quite well.

INTRODUCTION

In previous experiments in this series of studies of the deposition of magnetite particles from suspension in water onto heat exchange surfaces, deposition patterns were usually monitored for periods longer than about 50 hours (Callamand, Basset and Lister, 1999; Carpentier, McCrea and Lister, 2001) – in some cases up to about 700 hours (Basset et al., 2000). Thus, the long-term kinetics of deposition were established and the means of predicting fouling as a function of the operating parameters of the system were provided. For understanding the mechanisms, however, the initial period of fouling can be particularly important, since the first layers of particles to deposit affect the surface markedly, modifying it for the deposition of subsequent layers. The first few layers are therefore expected to deposit with kinetics different from those of the rest of the deposit. In water systems, a prime example arises from the change in electric charge on the surface of a heat exchanger tube at a certain pH as particles of a different point of zero charge (PZC) deposit. Initially, charge differences would create attractive forces and deposition would be promoted, in the extreme case limited only by transport in the fluid. Later, a thicker deposit would present similar charges to the particles and repulsive forces would impede deposition, in the extreme case limiting the process entirely through the particle-surface attachment term.

The scatter of the data in the deposition results from the early experiments often seems to contain a dip in the patterns that arise from a reduction of the deposition rate a few hours into the experiments (Carpentier, McCrea and Lister, 2001); Basset et al., 2000). As described later, we have reproduced this in a series of short experiments measuring the deposition of synthetic magnetite particles onto Alloy-800 heat exchanger tubing. The distinct knee in the accumulation curves that occurred at 5 – 10 hours can be described by the mechanism of an initial layer's modifying the surface for the deposition of subsequent layers.

EXPERIMENTAL METHODS AND APPARATUS

The magnetite particles used in the experiments were synthesised using a sol-gel technique first described by Sugimoto and Matijevic (1980). Monodispersed spheres were obtained; at about 0.4 μm diameter these were somewhat smaller than the 0.6 μm diameter particles of Basset et al. (2000). The magnetite was added to the coolant of a recirculating water loop that operated at about atmospheric pressure and at temperatures up to 90°C. Loop construction is mostly of stainless steel, comprising a 170 L reservoir equipped with a stirrer and electric heater, a centrifugal pump and a cooler. The test section is a vertical glass column, 1.5 m long and 9.4 cm I.D., with two outlet ports at the top. The Alloy-800 heat exchanger tube has a 1.6 cm OD and is cut to a length of 30 cm. It is inserted into the closure seal at the top of the test section. Heat fluxes up to 240 kW/m^2 can be generated in the tube by means of an internal electric heater.

During an experiment, samples of coolant were taken regularly and tested for pH and magnetite concentration, the latter via an atomic absorption spectrometer. Most of the experiments were done at neutral conditions but, when required, adjustments of pH were made with potassium hydroxide or nitric acid. Air was excluded from the coolant by continuous purging with nitrogen and magnetite concentration was adjusted by dilution or colloid addition.

The amount of deposit was measured by removing the tube from the glass column, dissolving the magnetite in dilute hydrochloric acid and measuring the iron concentration with atomic absorption. This provided an average surface concentration of magnetite on the Alloy-800.

Experiments were mostly carried out at 90°C bulk temperature in the column with a few runs at 60°C. Scoping tests to gauge the effects of system parameters on magnetite deposition measured the deposition velocity as the amount deposited after six hours exposure divided by the time (assumed to be the initial deposition rate) and by the bulk concentration of magnetite. The magnetite concentration in the loop was usually controlled between 4.0 and 4.5 μg/cm^3.

RESULTS

Many of the runs were carried out with a heat flux of 155 kW/m^2. At the highest coolant flow rate in the loop (13.5 L/min), giving a Reynolds number of 8,037 in the annular flow region of the test section, sub-cooled boiling was exhibited over most of the tube surface. The amount of boiling could be adjusted on the tube by increasing the heat flux or by lowering the flow rate while maintaining the heat flux at the original setting.

Deposition during boiling produced 0.1 mm – 0.2 mm diameter rings or spots of magnetite around the steam-bubble nucleation sites. These were similar to those described earlier (Basset et al., 2000) and are attributed to particle trapping and agglomeration on the growing bubble surfaces and to evaporation of the coolant micro-layers below the bubbles. Figure 1 is a composite scanning electron micrograph of a section through a typical ring along with its measured profile shown to scale.

The first set of experiments gauged the effect of bulk magnetite concentration on the deposition velocity. The results showed that the deposition velocity is approximately constant over the range of concentrations explored (0.112 – 48.5 μg/cm^3). This is consistent with previous findings, which found deposition rate to be approximately linear with concentration (Carpentier, McCrea and Lister, 2001); Basset et al., 2000).

Figure 2 presents the results of two sets of runs showing how deposition velocity varies over similar ranges of pH. The sets are in good agreement, both indicating a maximum deposition rate at about pH 7.5. This corresponds to the result of Basset et al (2000), who found the maximum deposition rate under similar sub-cooled boiling conditions to occur at pH 7.5 – 8.0. In a previous study under bulk boiling conditions, however, maximum deposition rates occurred at lower pH values, presumably because of local changes in the PZC of both the particles and the surface caused by local concentration of the chemistry additive (Carpentier, McCrea and Lister, 2001).

Figure 3 presents deposition velocity as a function of heat flux for otherwise constant conditions. As was found before (Basset et al., 2000), deposition was fairly constant below a heat flux of 40 kW/m^2, close to the value at which bubble nucleation began, and increased rapidly thereafter. Unlike the previous results, however, the variation with heat flux was more or less linear rather than parabolic. This may be due to the scatter of the data over the lower range of 0 – 194 kW/m^2, in contrast to repeated results over the range 0 – 240 kW/m^2 in the previous experiment. In any case, the curve is much flatter than expected from observations in previous experiments, which is probably the result of data scatter.

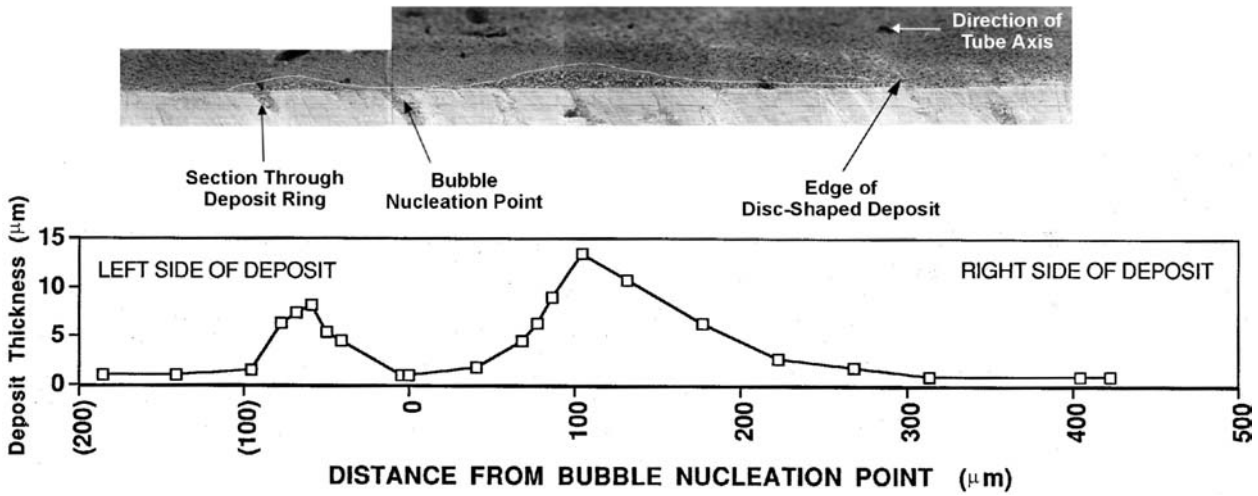

Figure 1. Composite scanning electron micrograph of a section through a magnetite ring formed at a bubble nucleation site.

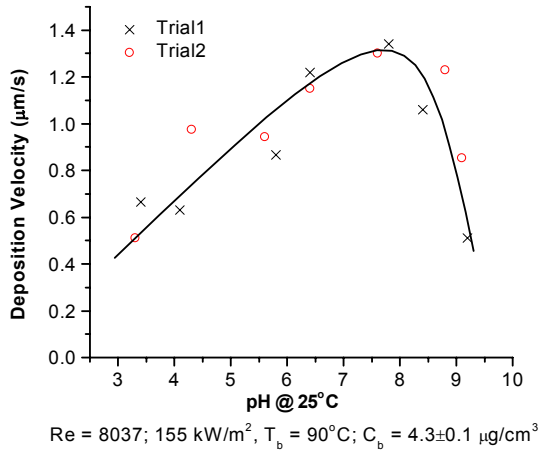

Figure 2. Variation of deposition velocity with $pH_{25°C}$.

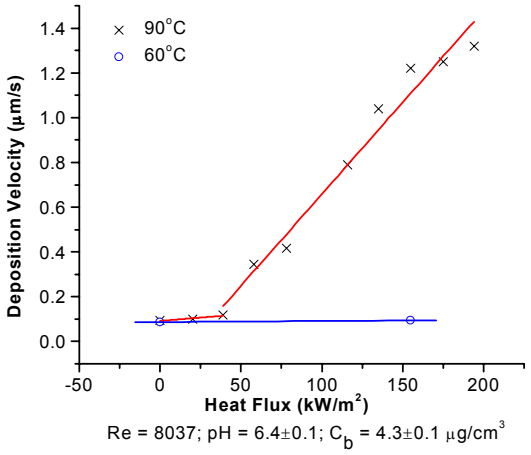

Figure 3. Variation of deposition velocity with heat flux.

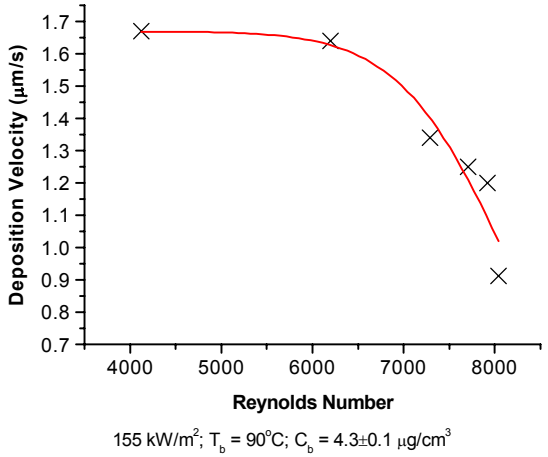

Figure 4. Variation of deposition velocity with Reynolds Number.

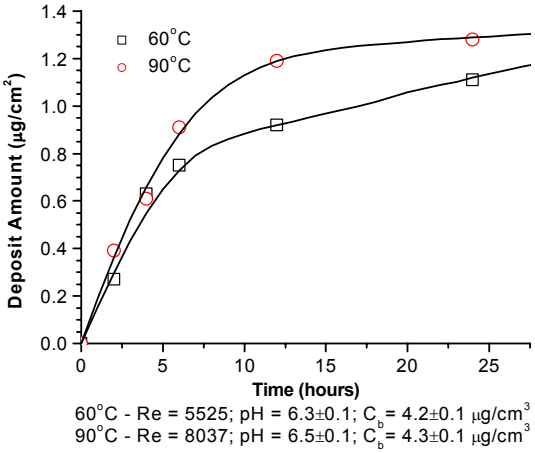

Figure 5. Variation of deposit with time under isothermal conditions at two bulk temperatures.

Figure 4 presents deposition velocity as a function of Reynolds number. The falling trend is due to the decreasing intensity of sub-cooled boiling as the pressure in the column increased in conjunction with an increase in flow rate. This effect was confirmed through a calculation of head losses in the system to obtain an estimate of the pressure in the column and the corresponding saturation and wall temperatures (calculated using the Jens and Lottes correlation, 1992).

Figures 5 and 6 show how deposition varies with time respectively under isothermal conditions and with heat flux; each figure contains plots for two different bulk temperatures at the column inlet – 60°C and 90°C – and curves for the fitted model (describe later) are included. All the curves show a distinct "knee" at 5 – 10 hours. Before the knee, the 60°C and 90°C data correspond for both the isothermal and subcooled boiling experiments; thereafter, the 60°C data are lower than the 90°C data. The deposition rates shown on the curves for the subcooled boiling experiments (i.e., with heat flux) are over an order of magnitude higher than those for the isothermal experiments.

Finally, Figure 7 shows how deposition under sub-cooled boiling conditions varies with time at both low pH and high pH. Both curves display a knee at 8 – 10 hours and the deposition amount at pH 8 is higher than at pH 4. While the latter observation is consistent with the effect of pH on deposition velocity as shown in Figure 2, the absolute values from the curves through the Figure 7 data at 6 hours (which define deposition velocity) are closer than anticipated, presumably because of the scatter in the data.

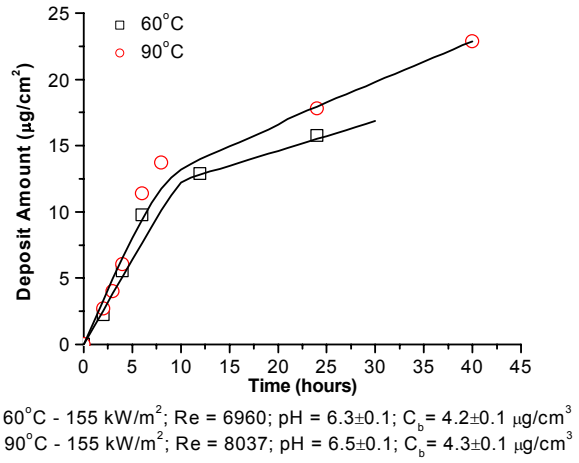

Figure 6. Variation of deposit with time at 155 kW/m^2 heat flux and two bulk temperatures.

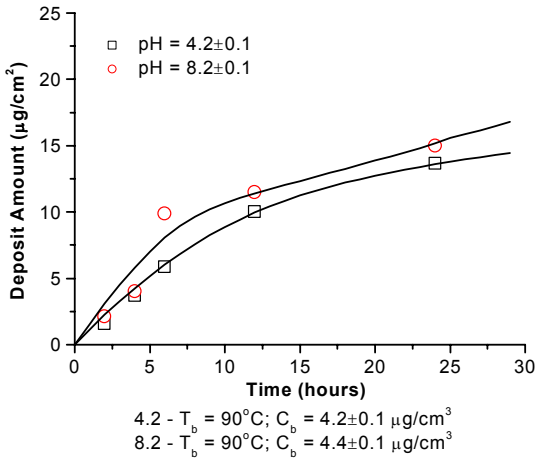

Figure 7. Variation of deposit with time at 155 kW/m^2 heat flux and two pH values.

THEORY AND DISCUSSION

The trends of deposition velocity with the operating parameters bulk concentration, heat flux and pH are similar to those recorded in earlier experiments, indicating that the 0.4 μm magnetite particles in these experiments behaved in a similar way to the 0.6 μm particles before. Thus, for most of the experiments, which were carried out at pH 6 – 7, the deposition rates are close to the maximum and resistance to particle deposition should have a large component due to transport in the fluid.

Since deposition depends linearly on concentration, C_b, we express the initial flux of depositing particles ϕ_l by:

$$\phi_l = C_b k_d \tag{1}$$

where k_d is the overall deposition coefficient (assumed to be equivalent to measured deposition velocity). For two deposition processes in series – transport of particles from the bulk to the wall followed by attachment – the overall coefficient is written as:

$$1/k_d = 1/k_t + 1/k_a \tag{2}$$

where k_t is the transport coefficient and k_a the attachment coefficient.

Under isothermal conditions:

$$k_t = 0.084\, u^* Sc^{-0.67} \tag{3}$$

where u* is the friction velocity ($\sqrt{\tau/\rho}$) and Sc the Schmidt number ($\mu/\rho D_p$) with τ the fluid shear stress at the wall, ρ the fluid density, μ the viscosity and D_p the particle diffusivity (Epstein, 1988).

Under non-isothermal conditions, such that the particles must diffuse against a temperature gradient, the transport coefficient is modified with a subtractive term k_{th}, the thermophoretic velocity:

$$k_t' = k_t - k_{th}/2 \tag{4}$$

where:
$$k_{th} = 0.26 \cdot \frac{1}{2\lambda_l + \lambda_p} \cdot \frac{\nu_l}{T} \cdot Q \tag{5}$$

in which λ_l and λ_p are the liquid and particle thermal conductivity, respectively, ν_l is the kinematic viscosity, Q the heat flux (W/m^2) and T the temperature (K) (Mηller-Steinhagen et al, 1988).

It should be noted that in boiling the evolution of bubbles disturbs the diffusion processes just described. Depending on the intensity of the boiling, deposition may be enhanced or impeded (Basset et al., 2000). An additive term, k_b, quantifying the boiling contribution to the transport coefficient in Equation 4, has been used and is similar to that described by Turner and Godin (1994).

To describe the initial processes of deposition, we assume that the attachment term in Equation 2 is complex, involving the attachment first of all of a primary layer and then subsequent layers that can be attached on top of the developing primary layer. The rate of attachment of primary particles, dN_1/dt, in terms of number concentration on the surface is given by, for $AN_1 < 1$:

$$\frac{dN_1}{dt} = k_1 N_w (1 - AN_1) \tag{6}$$

where k_1 is the attachment coefficient for primary particles at the wall, N_w is the number concentration in the liquid film at the wall and A is the effective area of a deposited particle.

Similarly, the rate of deposition of subsequent or secondary particles is given by:

$$\frac{dN_2}{dt} = k_2 \; N_w \; (AN_1) \tag{7}$$

where k_2 is the attachment coefficient for particles to themselves.

The transport of particles to the wall is given by:

$$\frac{dN_1}{dt} + \frac{dN_2}{dt} = k_t' \; (N_b - N_w) \tag{8}$$

where N_b is the number concentration in the bulk (note that number concentration is related to mass concentration via the mass of a particle, m; thus, $C_b = m\, N_b$). Assuming that the liquid film at the wall is at quasi steady state, N_w can be eliminated and Equations 6, 7 and 8 solved to give:

$$(k_1 - k_2)\, N_1 - \frac{(k_2 + k_t')}{A} \ln(1 - AN_1) = k_1 \; k_t' \; N_b \; t \tag{9}$$

and $$N_2 = \frac{k_2}{k_1 A}\left[\ln \frac{1}{(1 - AN_1)} - AN_1 \right] \tag{10}$$

At the start of the deposition:

$$\left.\frac{dN_1}{dt}\right|_{t=0} = \frac{k_1 \; k_t'}{(k_1 + k_t')} N_b \tag{11}$$

as expected for two processes in series.

At long times, at $t = \infty$, $N_1 = 1/A$, and:

$$\left.\frac{dN_1}{dt}\right|_{t=\infty} = 0 \qquad \text{and} \qquad \left.\frac{dN_2}{dt}\right|_{t=\infty} = \frac{k_2 k_t'}{(k_2 + k_t')} N_b$$

the latter also as expected for two processes in series.

Deposition curves such as those in Figures 5 – 7 can be interpreted in terms of these relations. The steep initial slope reflects the rapid deposition of the primary layer of particles onto the alloy surface while the shallower slope at the end reflects the deposition of particles onto an already fouled surface.

In order to extract the coefficients k_1 and k_2 from the data, we evaluate the transport coefficient k_t' for the conditions of the experiments via Equations 3 – 5. Once the experimental transport coefficient is obtained and the two attachment coefficients calculated for the given experimental condition, the effective area of the particles in the initial deposit layer can be determined through an iterative approach. The attachment coefficients and effective area term, as found for each experiment in this series, are given in Table 1. It should be noted that for the non-isothermal cases, the thermophoretic velocity term dominated, leading to negative values for the overall transport coefficient when Equation 4 was applied, as has been previously reported (Basset et al., 2000). This could be due to differences between our system and the system for which the correlation was derived. Evidence of this is given by Muller-Steinhagen et al. (1988) who reported lower deposition rates in boiling conditions, which is contrary to the results reported here and by Basset et al. thus, the thermophoresis expression clearly does not apply under the conditions in these experiments and has been omitted from the interpretation. For the experiments at 90°C with heat flux, sub-cooled boiling occurred over most of the tube surface and is accounted for by an empirical boiling coefficient, k_b, which is additive to the transport coefficient, k_t, in Equation 4; it is extracted from the deposition velocity versus heat flux curve in Figure 3 and values are reproduced in Table 1. We could not, however, use this treatment for the 60°C data because, as shown in Figure 3, the transition from non-boiling heat transfer to subcooled nucleate boiling had not yet occurred, as demonstrated by the low deposition.

The values calculated for the transport coefficient, k_t, for all experimental conditions, through Equation 3, are too low when compared with the experimental data. Basset et al (2000) and Turner and Godin (1994) have commented on this deficiency in the diffusion model before. Basset et al. were able to obtain better modelling results when applying the friction velocity, as calculated through the commercial fluid-dynamic code FLUENT and verified via Laser-Doppler anemometry (LDA), in Equation 3. Even with the modified friction velocity, the calculated transport coefficient was two to three times lower than those experimentally measured. Thus, the values for the transport coefficient used here have been modified by applying an appropriate factor to the friction velocity to make it correspond to the FLUENT and LDA results and doubling the coefficient in Equation 3 to 0.168, as suggested also by Basset et al.

Figures 8 and 9 depict the modelled growth of the primary and secondary deposit layers and the overall deposit for the isothermal and the subcooled boiling experiments at 90°C and near neutral pH. In all cases, the primary layer saturates in around 20 to 25 hours, after which time the overall deposition is completely controlled by the growth of the secondary layer.

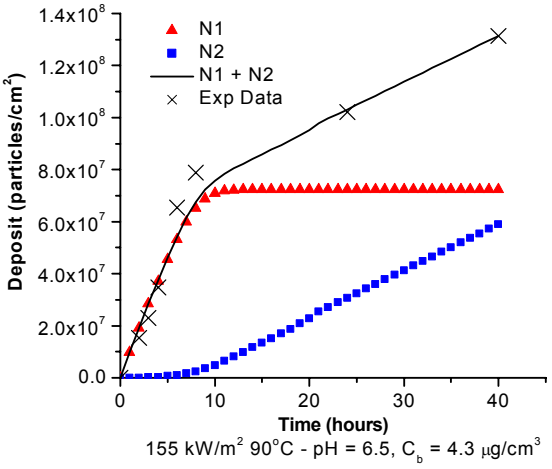

Figure 8. Modelling results applied to subcooled boiling condition.

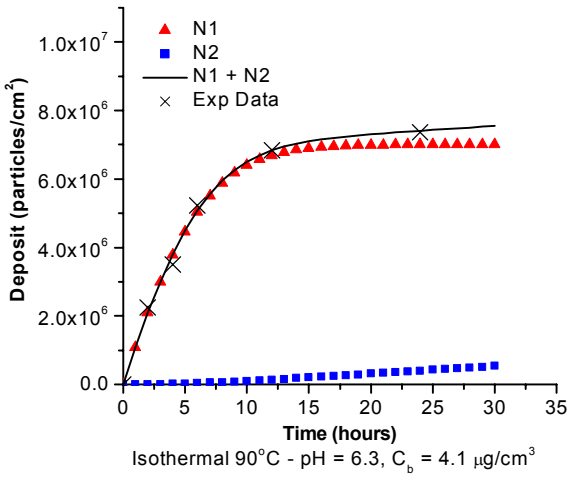

Figure 9. Modelling results applied to isothermal condition.

Table 1. Calculated model parameters.

	60°C		90°C			
	Isothermal pH = 6.3	**155 kW/m² pH = 6.3**	**Isothermal pH = 6.3**	**155 kW/m² pH = 4**	**155 kW/m² pH = 6.5**	**155 kW/m² pH = 8**
K_t' (cm/s)	1.36×10^{-5}	8.67×10^{-5}	2.30×10^{-5}	1.25×10^{-4}	1.25×10^{-4}	1.25×10^{-4}
K_b (cm/s)	--	--	--	9.91×10^{-5}	9.91×10^{-5}	9.91×10^{-5}
K_1 (cm/s)	4.43×10^{-5}	4.84×10^{-3}	2.73×10^{-5}	1.27×10^{-4}	1.02×10^{-3}	5.63×10^{-4}
K_2 (cm/s)	1.09×10^{-6}	1.78×10^{-5}	2.50×10^{-7}	7.98×10^{-5}	2.38×10^{-5}	2.30×10^{-5}
A (cm²/particle)	2.13×10^{-7}	1.42×10^{-8}	1.43×10^{-7}	9.90×10^{-9}	1.38×10^{-8}	1.81×10^{-8}

The proposed mechanism for multi-layered deposition, as presented above, represents our observations over short times. However, it is clear that if the measured and modelled trends were to continue, much lower total deposits than are actually seen in long but otherwise similar experiments (Basset et al., 2000) would result. This suggests that some other mechanism comes into play at times longer than the duration of these experiments, effectively increasing k_2. This would create a cusp or dip in a long-term deposition curve. Another possibility is that the experiments reported here are not fully compatible with the longer ones and that the dips discernible in the deposition data are part of the scatter – as usually assumed. The only apparent difference, however, is the particle size (0.4 μm in these and 0.6 μm in the longer experiments of Basset et al.), which seems unlikely to be responsible for such a change in the mechanism. Either way, the explanation is elusive.

The values of A, the effective projected area of a deposited first-layer particle, are interesting (see Table 1). Since a 0.4 μm-diameter particle has a geometric projected area of 1.26×10^{-9} cm², its area of influence on the metal surface is an order of magnitude larger under boiling conditions and two orders larger under isothermal conditions. An area of influence two orders of magnitude larger than the actual projected area may be somewhat unrealistic, but it is possible that the characteristics of the entire heat exchange surface may be modified by a dispersion of evenly spaced particles. It is noteworthy also that the A values are fairly consistent during boiling, while increasing slightly with pH, and under isothermal conditions, while decreasing slightly with temperature.

The values calculated for the transport, boiling and two attachment coefficients are interesting as well. The transport coefficient, k_t', shows a slight increase with temperature – as expected through the diffusion model – and is increased by almost an order of magnitude with the addition of the boiling coefficient. The primary layer attachment coefficient, k_1, does not exhibit a large temperature effect in the isothermal cases but is significantly increased with boiling. Also notable is the trend of k_1 with pH – its value follows quite nicely the trend of deposition observed in Figure 2. Unlike the primary

attachment coefficient, the secondary attachment coefficient, k_2, is almost an order magnitude lower at the higher temperature in the isothermal case, while still showing a similar trend with pH as does k_1.

SUMMARY AND CONCLUSIONS

The results of these short-term experiments, which demonstrated a knee in the particle deposition data at about 10 hours, are satisfactorily modelled in terms of an initial layer of particles depositing with characteristic kinetics of attachment and modifying the surface so that subsequent layers deposit with different kinetics. Thermophoresis is ignored in the modelling of particle transport to the surface because a correlation for its effect leads to a prediction of negative deposition. To account for sub-cooled boiling, an empirical coefficient is deduced from the data and added to the diffusive transport term.

While the experiments provide a reasonably consistent set of results, extrapolating their deposition data to long times would produce thinner deposits than have been seen before in long experiments. Either a change in mechanism occurs to increase deposition rates after the subsequent particle layers are well established, or these experiments are not compatible with the longer ones. The apparent dips in the data of the longer experiments are then probably part of the scatter.

NOMENCLATURE

- A effective area of influence of a primary layer particle (cm^2/particle)
- C_b bulk concentration of magnetite in suspension ($\mu g/cm^3$)
- D_p particle diffusivity (cm^2/s)
- k_1 attachment coefficient for primary layer particles (cm/s)
- k_2 attachment coefficient for second layer particles (cm/s)
- k_a attachment coefficient (cm/s)
- k_b boiling coefficient (cm/s)
- k_d overall deposition coefficient (cm/s)
- k_t' modified transport coefficient (cm/s)
- k_t transport coefficient (cm/s)
- k_{th} thermophoretic velocity (cm/s)
- N_1 amount of primary layer particles deposited (particles/cm^2)
- N_2 amount of second layer particles deposited (particles/cm^2)
- N_b number of particles in bulk fluid (particles/cm^3)
- N_w number of particles at the tube surface (particles/cm^3)
- Q heat flux (W/m^2)
- Sc Schmitt Number – ($\mu/\rho D_p$)
- u* friction velocity - $\sqrt{\tau/\rho}$ (cm/s)
- ϕ_1 initial flux of depositing particles (particles/cm^2)
- λ_l fluid thermal conductivity (W/m.K)
- λ_p particle thermal conductivity (W/m.K)
- τ shear stress at the wall ($g\ cm/s^2cm^2$)
- ρ fluid density (g/cm^3)
- μ fluid dynamic viscosity (g/cm.s)
- ν fluid kinematic viscosity (cm^2/s)

ACKNOWLEDGMENTS

The authors would like to thank Mark Thorne who performed much of the experimental work, the Natural Sciences and Engineering Research Council of Canada for financial support and Dr. Carl Turner for his valuable insight and input.

REFERENCES

Basset, M., McInerney, J., Arbeau, N. and Lister, D.H., 2000, The Fouling of Alloy-800 Heat Exchange Surfaces by Magnetite Particles, *Can. J. Chem. Eng*., vol. 78, pp. 40-52.

Callamand, S., Basset, M. and Lister, D.H., 1999, Numerical Simulation of Corrosion Product Deposition on Heat Exchanger Surfaces, *Proc. Int. Conf. on Mitigation of Heat Exchange Fouling and its Economic and Environmental Implications.*

Carpentier, H., McCrea, L. and Lister, D.H., 2001, Deposition of Corrosion Product Particles onto Heat Exchange Surfaces in Bulk Boiling, *Proc. Int. Conf. on Heat Exchanger Fouling*, Davos, In press.

Epstein, N., 1988, Particulate Fouling of Heat Transfer Surfaces: Mechanisms and Models, L. F. Melo et al, Editors, *Fouling Science and Technology*, Kluwer Academic Publ., Dordrecht, Netherlands, pp. 143-164.

Jens, W.H and Lottes, P.A. 1992, Analysis of Heat Transfer, Burnout, Pressure Drop, and Density Data for High Pressure Water, extracted from *Steam – Its Generation and Use*, 40th Edition, Babcox & Wilcox.

Mηller-Steinhagen, H., Reif, F., Epstein, N. and Watkinson, A.P., 1988, Influence of Operating Conditions on Particulate Fouling, *Can. J. Chem. Eng.*, vol. 66, pp. 42.

Sugimoto, T. and Matijevic, E., 1980, Formation of Uniform Spherical Magnetite Particles by Crystallization from Ferrous Hydroxide Gels, *J. Colloid and Interface Sci*., vol. 74, no. 1.

Turner, C.W., 1993, Rates of Particle Deposition From Aqueous Suspensions in Turbulent Flow; A Comparison of Theory with Experiment, *Chem. Eng. Sci.*, vol. 48, pp. 2189-2195.

Turner, C.W. and Godin, M., 1994, Mechanisms of Magnetite Deposition in Pressurized Boiling Water and Non-Boiling Water, *Proc. 2nd Int. Steam Gen. and Heat Exch. Conf*., Toronto, Canada, Can. Nucl. Soc., pp. 111-123.